Title

Regulators of mitochondrial quality control differ in subcutaneous fat of metabolically healthy and unhealthy obese monkeys

Journal

Obesity, 25(4)

ISSN

1930-7381

Authors

Kavanagh, Kylie
Davis, Ashley T
Peters, Diane E
et al.

Publication Date

2017-04-01

DOI

10.1002/oby.21762

Peer reviewed

HHS Public Access

Author manuscript

Obesity (Silver Spring). Author manuscript; available in PMC 2017 August 25.

Published in final edited form as:

Obesity (Silver Spring). 2017 April ; 25(4): 689–696. doi:10.1002/oby.21762.

Regulators of Mitochondrial Quality Control Differs in Subcutaneous Fat of Metabolically Healthy and Unhealthy Obese Monkeys

Kylie Kavanagh[1], **Ashley T Davis**[1], **Diane E Peters**[1], **Andre Le Grand**[2], **Manish S Bharadwaj**[3], and **Anthony JA Molina**[3]

[1]Wake Forest School of Medicine, Department of Pathology, Wake Forest University Health Sciences, Winston-Salem, NC, USA 27157

[2]Wake Forest School of Medicine, Animal Resources Program, Wake Forest University Health Sciences, Winston-Salem, NC, USA 27157

[3]Wake Forest School of Medicine, Internal Medicine, Wake Forest University Health Sciences, Winston-Salem, NC, USA 27157

Abstract

Objectives—Obesity exists with and without accompanying cardiometabolic disease, termed metabolically unhealthy obesity (MUO) and healthy obesity respectively (MHO). Underlying differences in the ability of subcutaneous (SQ) fat to respond to nutrient excess is emerging as a key pathway. We aimed to document the first spontaneous animal model of MHO and MUO and differences in SQ adipose tissue.

Methods—Vervet monkeys (*Chlorocebus aethiops*; n=171) were screened for Metabolic Syndrome. A subset of MHO and MUO monkeys (n=6/group) had SQ fat biopsies collected for histologic evaluations and examination of key mitochondrial proteins.

Results—Obesity was seen in 20% of monkeys, and within this population, 31% were healthy which mirrors human prevalence estimates. MUO monkeys had more than 60% lower adiponectin concentrations despite similar fat cell size, uncoupling protein 3, and activated macrophage abundance. However, alternatively activated/anti-inflammatory macrophages were 70% lower. Deficiencies of 50% or more in mitochondrial quality control regulators, and selected mitochondrial fission and fusion markers were observed in the SQ fat of MUO monkeys despite comparable mitochondrial content.

Conclusions—We characterized a novel and translatable spontaneously obese animal model of healthy and unhealthy obesity, occurring independently of dietary factors. Differences in

Contact information: Kylie Kavanagh, Department of Pathology, Section on Comparative Medicine, Wake Forest University Health Sciences, Medical Center Blvd., Winston-Salem, NC 27127, U.S.A., Phone: (336) 713-1475, FAX: (336) 716-1515, kkavanag@wakehealth.edu.

Conflicts of Interest: No conflicts of interest exist for any author.

mitochondrial quality and inflammatory cell populations of subcutaneous fat may underpin divergent metabolic health.

Keywords

healthy obesity; vervet monkey; mitochondria; macrophage polarization

Introduction

The current obesity epidemic in developed nations is largely responsible for increases in diabetes and cardiometabolic disease prevalence. However, a significant proportion of obese persons do not have elevated traditional metabolic syndrome (MetSyn) risk factors (elevated blood pressure, glucose, triglycerides [TG], or low high-density lipoprotein cholesterol)(1, 2). Metabolically healthy obesity (MHO) is a conceptual description whereby an individual is classified as obese by standard body mass index criteria (> 30kg/m^2 in Caucasians) but lacks these measurable metabolic disturbances. The prevalence of MHO individuals is estimated to be as high as 35% in the U.S (1). Even overweight individuals are almost equally likely to be healthy as unhealthy, suggesting that obesity as a risk factor is not sensitive or specific for health outcomes. The risk for MetSyn development in people is complicated by variable dietary, genetic, and environmental exposures. Twin studies have aimed to reduce these factors, and one study has isolated subcutaneous (SQ) adipose tissue health and its ability to expand as being determinant for whether ectopic fat accumulates (3), and the subsequent generation of metabolic disease that is known to occur with fat accumulation in the liver and intra-abdominal space (4). There is controversy regarding the MHO state as to whether MHO confers long-term protection, or if it just delays from cardiometabolic disease development (5–7). This controversy centers around whether MHO is just a transient state that precedes the eventual and inevitable development of metabolic disease (5, 6), or whether these people represent a preferred biological handling of excess nutrient consumption and adipose tissue mass (8). Understanding the mechanisms behind MHO may aid in identifying populations at-risk for disease, and uncover new targets to treat MUO.

The biology of different adipose depots is an area of continuing high interest with pathways involving immune and inflammatory cell types emerging as being relevant in SQ fat (9). Recent data demonstrates that enhanced mitochondrial activity in adipose results in greater triglyceride accumulation, and if this expansion occurs in SQ adipose tissue, there is protection from metabolic disease (10). However, these observations from genetically manipulated rodents have yet to be observed in human or non-human primates. Moreover, potential differences between MHO and MUO adipose tissue mitochondria have yet to be determined. Vervet monkeys demonstrate spontaneous obesity, including intra-abdominal fat accumulation which is generally associated with insulin resistance and eventual T2DM development (11–14). We hypothesized that MHO and MUO is a conserved phenotype in non-human primates and would be observable despite lack of obesogenic lifestyle factors such as Western type diets and sedentary behavior. We identify unhealthy lean and obese monkeys, and describe the characteristics of SQ adipose from monkeys classified as healthy

or unhealthy obese, demonstrating that health status relates to differences in mitochondrial quality control regulators and inflammation.

Methods

Animals

African green monkeys (male and female vervet monkeys; *Chlorocebus aethiops*; n=171 Table 1) ranging in age from 9–27 years (maximum lifespan typically ≈ 25 years) were evaluated. This age range was selected to represent the ages when peak adiposity develops and type 2diabetes (T2DM) is typically diagnosed. The mean age of the cohort approximates a 60 year old human. Animals were housed in large indoor/outdoor enclosures that provide elevated perches and climbing structures within multigenerational social groups and *ad libitum* opportunities to socialize, eat, and exercise. A commercial laboratory primate chow (Laboratory Diet 5038; LabDiet, St. Louis, MO; Supporting Information Table S1) with supplemental fresh fruits and vegetables was fed once per day. All animal procedures were performed on a protocol approved by the Wake Forest University Institutional Animal Care and Use Committee according to recommendations in the Guide for Care and Use of Laboratory Animals (Institute for Laboratory Animal Research) and in compliance with the USDA Animal Welfare Act and Animal Welfare Regulations (Animal Welfare Act as Amended; Animal Welfare Regulations).

Experimental Design

Monkeys were assessed for general health by clinical examination three times annually, with blood collection and blood pressure measured once each year. Six females defined as MHO and MUO were randomly selected from females that were matched on age, waist, BMI, and BW. ***Procedures*** Animals were fasted overnight and anesthetized with intramuscular ketamine (10 to 15 mg/kg) to allow for sample and morphometric data collections. Each animal was weighed and waist circumference measured with a flexible tape measure at the level of the umbilicus. Body length was measured from the crown of the head to the caudal aspect of the pubic bone which is the equivalent to sitting height. A body mass index (BMI) was calculated by dividing the weight (kg) by the body length (m) squared. To ensure accurate classification as lean or obese, three consecutive measures over the period of 1 year were averaged for bodyweight, waist, and BMI. Triplicate measures of blood pressure (systolic and diastolic blood pressure [SBP and DBP]) were measured indirectly by high definition oscillometry at the tail base, and the average value reported. Blood samples were obtained by venipuncture of the femoral vein after an overnight fast and collected into ethylenediaminetetraacetic acid (EDTA) and serum separator blood tubes. The blood was held on ice until it could be processed. After processing the plasma and whole blood, samples were stored at −80°C until analysis. A subset of MHO and MUO monkeys had a subcutaneous (SQ) adipose tissue biopsy collected from the para-umbilical region and tissue was both fixed and processed for immunohistochemistry, and frozen in liquid nitrogen for protein extraction and western blotting.

Measurements

Fasting blood glucose was determined by the glucose oxidase method, and fasting plasma insulin and adiponectin concentrations were determined by enzyme linked immunosorbent assay (ELISA) (Mercodia, Uppsala, Sweden) from the plasma sample. Homeostasis model assessment (HOMA) was determined by the product of glucose and insulin divided by 22.5 and used to evaluate insulin resistance (15). Triglyceride (TG), high density lipoprotein cholesterol (HDLC) and total plasma cholesterol (TPC) concentrations were measured enzymatically. Circulating branched chain amino acid concentrations were measured in plasma by NMR spectroscopy (LabCorp, Raleigh NC). Circulating c-reactive protein (CRP, Alpco, Salem NH) and interleukin-6 (IL-6, R&D Systems, Minneapolis MN) were measured by ELISA from a subset of monkeys described below.

Metabolic syndrome (MetSyn) risk was defined as for the Adult Treatment Panel III criteria that were standard for TG (>150 mg/dL), blood pressure (>135/>85 mmHg for SBP and DBP respectively) and HDLC values for women (<50 mg/dL). Monkey-specific values were used for waist circumference and glucose. Obesity was defined as waist circumference > 40.5 cm (11) and the glucose threshold was set at 100 mg/dL which is consistent with lower fasting glucose values measured when primates consume diets that are free of simple carbohydrates and saturated fat (11). Risk scores were the sum of the number of values that exceeded the criteria cut-offs.

Adipose Tissue

Biopsied adipose tissue was washed with phosphate buffered saline and protein extracted by homogenization on ice in radioimmunoprecipitation assay buffer. The homogenate was centrifuged at 10,000 g for 5 minutes at 4°C and supernatant collected and stored until further analysis. Protein concentration was determined by the bicinchoninic acid protein assay and equal amount of protein were separated by 12% sodium docyl sulfate polyacrylamide gels. Separated proteins were electrophoretically transferred onto a nylon polyvinylidene fluoride (PVDF) membrane and blocked at room temperature for 60 minutes with either 5% non-fat milk or bovine serum albumin with 0.1% Tween 20 in Tris-buffered saline. Membranes were probed with commercially available primary antibodies to: VDAC (porin) antibody (1:1000), COX IV (1:10,000), mitofusin-1 (mfn1) (1:1000), mitofusin-2 (mfn2) (1:1000), optic atrophy 1 (Opa1) (1:1000), mitochondrial fission protein (Fis1) (1:500), peroxisome proliferator-activated receptor gamma coactivator one (PGC1)alpha (1:1000), silent mating type information regulation 2 homolog (SIRT)1 (1:1000), SIRT3 (1:1000), mitochondrial transcription factor A (TFAM) (1:2000), heat shock protein (HSP)70 (1:1000), dynamin-related protein (DRP)1 (1:500) (Abcam Inc, Cambridge, MA); pink-1 (1:2000) and parkin (1:2000) (Cell Signaling Technology, Inc., Danvers, MA), and uncoupling protein (UCP)3 (1:1000) (GeneTex Inc, Irvine, CA). Appropriate horseradish peroxidase (HRP)-conjugated secondary antibodies were added and immunoreactive proteins were then visualized using the Supersignal West-Pico Chemiluminescent reagent (Thermo Scientific, Rockford, IL). Gyceraldehyde 3-phosphate dehydrogenase (GAPDH) antibody (1:2000) (Abcam Inc, Cambridge, MA) was used as a loading control. The density of each immunoreactive product was quantified using a Kodak Imaging system (Kodak,

Rochester, NY) and normalized to GAPDH. Representative western blot images are shown in Supporting Information Figure S1.

Histology

Histological sections were created from paraffin embedded adipose tissues. Adipocyte size was measured by 200 individual cell diameters being calculated from 10 representative fields viewed at the 10× magnification level with 20 adjacent cell diameters recorded per field. Average cell diameter was calculated and reported. Immunohistochemistry stains were applied to identify classically activated M1 macrophages (pan-macrophage marker CD68 [AbD Serotac Bio-Rad, Raleigh NC), and alternatively (M2) activated macrophages (CD163 [Thermofisher, Rockford IL). CD68 positive cell staining was counted in triplicate, across 15 fields at 40× magnification and all perivascular smooth muscle cells were excluded. CD163 positive cell staining was infrequent and so cells were manually counted from the entire biopsy sample and normalized to the total area of the biopsy piece. A ratio of M2/M1 measurements were calculated and reported. Identification of these cell types is complex, and markers chosen here represent a basic delineation of macrophages, and CD163 staining alters in concert with changes in the metabolic status of people (16). All histological assessments were conducted by persons blinded to the identity of the samples.

Data Analysis

Statistical analyses were performed using Statistica v.10 (StatSoft, Tulsa, OK) and p values of ≤ 0.05 were considered significant. Logarithmic transformation was applied to endpoints not meeting normality assumptions. Metabolic and phenotypic variables were analyzed for differences by analysis of variance.

Results

Population screening

Despite no influence of high dietary saturated fat, cholesterol, salt, or simple carbohydrate excess, there is a natural diversity of metabolic health in these middle-aged to older monkeys (Table 1). MetSyn risk criteria were observed at high frequencies in our monkey population (Figure 1A). One fifth of the animals assessed had central obesity, high glucose, high blood pressure, and/or low HDLC. These risk factors overlapped within individuals such that the population divided approximately evenly into thirds being free of metabolic syndrome risk, having only one risk factor and being high risk with 2 or more of the 5 MetSyn criteria (Figure 1B). We see very clear delineation of healthy and unhealthy monkeys in both the normal and obese populations (Table 1). Metabolically unhealthy individuals were present in both the normal and obese populations (Figure 1C) and mirror the proportions observed in the US population where 32% of people with obesity were classified as metabolically healthy (1). As this population is consuming a low-fat, cholesterol- and simple carbohydrate diet (Supporting Information Table S1) the differences seen in MetSyn risk criteria are of high interest. Obesity resulted in higher glucose, insulin and HOMA values whereas lipid parameters and blood pressure were less affected. Impaired fasting glucose ([IFG] >110 mg/dL) was frequently observed in monkeys classified as unhealthy based on their metabolic syndrome score (29% of unhealthy obese and 52% of unhealthy lean monkeys). In monkeys

classified as healthy, obese monkeys had greater prevalence of IFG than lean monkeys (18% versus 3%). Being classified as metabolically unhealthy, regardless of obesity, exaggerated glucose values such that overall these monkeys were classified with impaired fasting glucose. Systolic blood pressure was on average 19% higher in unhealthy monkeys when compared to the healthy monkeys.

Subset of MHO and MUO monkeys

The monkeys sampled for subcutaneous fat were representative of MHO and MUO (Figure 2A and B, Table 2). Adiponectin concentrations were 41% lower in metabolically unhealthy monkeys than healthy monkeys, suggesting altered adipocyte function despite their comparable adiposity (Figure 2C). Lower adiponectin was not related to differences in fat cell size, or fat type as average cell diameter and UCP3 protein levels were comparable (Table 2; Supporting Information Figure S2A). Classically activated macrophages (M1, $CD68^{+ve}$) were present in both groups and numerically higher in the MUO (25% greater) but the variability was high. However, alternatively activated anti-inflammatory macrophages (M2, $CD163^{+ve}$) were more sparse in adipose tissue from MUO monkeys, on average 70% lower abundance (Table 2; Supporting Information Figure S2B and C), leading to a dramatic re-distribution of the M1/M2 balance in adipose from healthy and unhealthy obese monkeys (Figure 2D). Local changes in adipose inflammatory cell balance was not reflected in generalized inflammatory burden as measured by circulatory IL-6 and CRP levels (Table 2).

The expression of proteins involved in mitochondrial quality control was lower in MUO (Figure 3). Pink1, parkin and its chaperone HSP70 are associated with mitophagy and were uniformly deficient in MUO individuals. Further, reductions in DRP1 and Mfn2 indicate potential defects in mitochondrial fission and fusion respectively in SQ adipose from MUO monkeys (Table 3). Whereas mitochondrial quality control markers were clearly deficient in MUO, the expression of other markers of fission (FIS1) and fusion (OPA1 and Mfn2) were not different. These changes were seen in the absence of differences in the expression of two independent reporters of mitochondrial content (porin and COXIV; Table 3). Notably, all markers of content and biogenesis were numerically reduced in “unhealthy” adipose. Branched chain amino acids in circulation were comparable (Supporting Information Table S2).

Discussion

Our evaluation of vervet monkeys establishes MHO and MUO as distinct health phenotypes that are conserved within primates, and that dietary etiologies are not underpinning the development of these states. Further, we demonstrate that non-obese monkeys similarly demonstrate both good and poor metabolic health status. This is the first report describing spontaneous MUO and MHO in an animal model, and moreover a primate model which spontaneously develops type 2 diabetes and cardiovascular disease with aging (17, 18). The prevalence of MUO is strikingly similar to that reported in people, however the prevalence of metabolically unhealthy lean monkeys was much lower (12% versus 30% in people) (1). We would predict that exposure of monkeys to a typical Western diet may unmask individual susceptibility to metabolic disease and that this proportion of lean unhealthy monkeys would

increase (19, 20). We show that MUO monkeys have altered subcutaneous adipose tissue function with reduced circulating adiponectin concentrations, a pro-inflammatory macrophage distribution, and indicators that mitochondrial quality control mechanisms are disturbed. These are novel findings attributed to MUO fat and seen in the absence of changes in adipose cell size, total macrophage content and systemic inflammation.

One prevailing theory regarding MHO is the subcutaneous expandability theory whereby the ability for SQ adipose to increase triglyceride storage is related to good health status, as fat remains out of liver and muscle tissues which are ectopic sites known to drive insulin resistance (3, 4). However in contrast to this theory, profiling gene expression in SQ fat of people with obesity found that healthy obese individuals had lower transcripts of matrix metalloproteinase 9, which is unexpected as this enzyme is key in extracellular matrix remodeling which allows fat expansion and neovascularization (9). This study did however identify up regulation of genes involved in immune and inflammatory pathways in unhealthy obese subjects which is consistent with our documentation of shifted macrophage polarization. Macrophage polarization in people with obesity has been shown to be similar in SQ and visceral fat depots, and macrophage type shifts towards a healthier ratio with weight loss (and concomitant improvements in health status) (16). The interaction between tissue remodeling and fat expansion and inflammation has been linked recently through macrophage-derived interferon regulator factors (Irf's). Irf's are secreted from M1 macrophages and activate inflammatory pathways, which in turn reduce transforming growth factor-β which is required for normal remodeling. Obese mice and humans have more Irf5 in adipose which functions in a paracrine fashion to limit remodeling and collagen depositions, and is associated with insulin resistance development (21). These factors involved in fat remodeling, and related collagen and capillary elements, were not evaluated in our monkeys SQ adipose tissue and represent another avenue of investigation that looks likely to be relevant.

Our study of MHO and MUO shows adipose tissues have similar cell sizes and small differences in M1 macrophages, and was without dramatic differences in tissue appearance but there were changes in inflammatory profiles as measured by adiponectin and M2 macrophage content. There is little data about M2-polarized macrophages in adipose tissues to date, but they do have the capacity to change their abundance in adipose tissue and have been seen to increase in number concurrent with improved health profiles (16, 21). Lower inflammation as measured by circulating cytokines and adipokines has been consistent in multiple studies of human healthy obesity (22, 23). This shift in inflammatory profile is related to higher inflammasome activation in visceral fat of unhealthy people with obesity (24). There is recent evidence being generated that links macrophage-driven inflammation by inflammasome activation with mitochondrial dysfunction. Inflammasome activation is dependent on mitochondrial transport and normal mitophagy. When mitochondrial function becomes dysfunctional, it likely drives pro-inflammatory tissue responses (25, 26). Our data indicates that adipose tissue changes and MetSyn risk are coupled, and can exist without increases in circulating cytokine concentrations. We believe this suggests that AT changes underpin early changes in cardiometabolic risk and that inflammation arises secondary to greater macrophage accumulation within fat (14, 27). A number of studies evaluating mitochondria sourced from adipose tissue in metabolic disease have observed differences in

total mitochondrial content, compromised respiratory capacity or greater oxidative stress (28, 29). Biomarkers that suggest differences in mitochondrial function have been observed in the metabolically healthy and unhealthy obese adipose when assessed by transcription profiling of human fat (9). Manipulation of mitochondrial electron transport activity in fat tissues of rodents specifically modulates adiponectin production and overall metabolic health following high fat diets and weight gain (10) which supports the concept that mitochondrial health is upstream of inflammatory and metabolic effects on adipose tissue. Obese mice have altered mitochondrial morphology and function without changes mitochondrial protein levels that are seen in diabetic mice (28, 30). In our monkeys, we see evidence of disrupted mitochondrial quality control but abundance markers are comparable or non-significantly lower. These findings highlight the need for future studies evaluating mitochondrial function/bioenergetics and in the regulation of mitochondrial turnover, such as parkin mediated ubiquination and degradation.

Parkin is an E3 ubiquitin ligase that regulates c-jun N-terminal kinase (JNK) activity via the requisite ubiquination of HSP70 (31). HSP70 is cytoplasmic chaperone protein that we have documented in this same monkey model as being determinant of metabolic health over time when measured in skeletal muscle, which is a mitochondrially rich tissue (32). The importance of parkin/HSP70 has been replicated in mouse models lacking HSP70 and myotubes lacking Parkin (33). In these studies the initiating factor for parkin/HSP70 activity was depolarized mitochondria which recruits HSP70, and in turn regulates Parkin activity. If this process was disrupted, JNK activation and insulin resistance of the muscle resulted. Our study supports this process with low Parkin/HSP70 in SQ adipose being associated with insulin resistance and MetSyn. It is unknown whether suggests that inadequate Parkin/HSP70 in SQ adipose tissue results in the accumulation of damaged mitochondria, or if chronic metabolic stress leads to the down-regulation of HSP70 which has been seen in this monkey and other animal models of hyperglycemia and/or hyperinsulinemia (34, 35). In our study of fat, HSP70 and Parkin had largest numerical difference between MHO and MUO tissues, thus therapies to restore HSP70 in the MUO may be an effective strategy to shift MUO towards MHO.

Our study is a first in defining the spontaneous development of divergent metabolic health status in both lean and obese monkeys. Limitations of this study are the underrepresentation of males that results from screening of adults within a breeding colony, and the lack of imaging based assessments that would permit the quantification of all fat depots. We present a truly translational model that can be used to answer many gaps in knowledge that exist regarding the underlying causes of obesity-related MetSyn. The biology demonstrated in the fat tissue of these monkeys and the importance of normal mitochondrial function in rodent models (10, 25, 26, 28, 30, 36) suggest that reduced mitochondrial quality control may be a primary deficit in SQ adipose of MUO and result in inflammation and reduced adiponectin. What is unknown is whether these deficiencies are present in all adipose depots and insulin sensitive tissues, or if mitochondrial quality control, mitophagy, and inflammation changes with interventions such as weight loss, HSP70 induction, or if the MHO actually accrues greater dysfunction over time. As the obesity epidemic continues to spread globally without evidence to suggest reversal (37), understanding the underlying biology that protects an individual from MetSyn is of continued importance.

Supplementary Material

Refer to Web version on PubMed Central for supplementary material.

Acknowledgments

Funding: Funding sources for this work came from NIH P40 OD010965 and Wake Forest School of Medicine.

References

1. Wildman RP, Muntner P, Reynolds K, McGinn AP, Rajpathak S, Wylie-Rosett J, et al. The obese without cardiometabolic risk factor clustering and the normal weight with cardiometabolic risk factor clustering: prevalence and correlates of 2 phenotypes among the US population (NHANES 1999–2004). Arch Intern Med. 2008; 168(15):1617–1624. [PubMed: 18695075]
2. Grundy SM, Neeland IJ, Turer AT, Vega GL. Ethnic and gender susceptibility to metabolic risk. Metab Syndr Relat Disord. 2013; 12(2):110–116. [PubMed: 24325736]
3. Naukkarinen J, Heinonen S, Hakkarainen A, Lundbom J, Vuolteenaho K, Saarinen L, et al. Characterising metabolically healthy obesity in weight-discordant monozygotic twins. Diabetologia. 2013; 57(1):167–176. [PubMed: 24100782]
4. Fabbrini E, Magkos F, Mohammed BS, Pietka T, Abumrad NA, Patterson BW, et al. Intrahepatic fat, not visceral fat, is linked with metabolic complications of obesity. Proc Natl Acad Sci U S A. 2009; 106(36):15430–15435. [PubMed: 19706383]
5. Aung K, Lorenzo C, Hinojosa MA, Haffner SM. Risk of developing diabetes and cardiovascular disease in metabolically unhealthy normal-weight and metabolically healthy obese individuals. J Clin Endocrinol Metab. 2014; 99(2):462–468. [PubMed: 24257907]
6. Mongraw-Chaffin M, Foster MC, Kalyani RR, Vaidya D, Burke GL, Woodward M, et al. Obesity severity and duration are associated with incident metabolic syndrome: Evidence against metabolically healthy obesity from the Multi-Ethnic Study of Atherosclerosis. J Clin Endocrinol Metab. 2016 jc20162460.
7. Ryden M, Hrydziuszko O, Mileti E, Raman A, Bornholdt J, Boyd M, et al. The Adipose Transcriptional Response to Insulin Is Determined by Obesity, Not Insulin Sensitivity. Cell Rep. 2016; 16(9):2317–2326. [PubMed: 27545890]
8. Fabbrini E, Yoshino J, Yoshino M, Magkos F, Tiemann Luecking C, Samovski D, et al. Metabolically normal obese people are protected from adverse effects following weight gain. The Journal of clinical investigation. 2015; 125(2):787–795. [PubMed: 25555214]
9. Das SK, Ma L, Sharma NK. Adipose tissue gene expression and metabolic health of obese adults. International journal of obesity. 2015; 39(5):869–873. [PubMed: 25520251]
10. Kusminski CM, Holland WL, Sun K, Park J, Spurgin SB, Lin Y, et al. MitoNEET-driven alterations in adipocyte mitochondrial activity reveal a crucial adaptive process that preserves insulin sensitivity in obesity. Nat Med. 2012; 18(10):1539–1549. [PubMed: 22961109]
11. Kavanagh K, Fairbanks LA, Bailey JN, Jorgensen MJ, Wilson M, Zhang L, et al. Characterization and heritability of obesity and associated risk factors in vervet monkeys. Obesity (Silver Spring). 2007; 15(7):1666–1674. [PubMed: 17636084]
12. Kavanagh K, Jones KL, Sawyer J, Kelley K, Carr JJ, Wagner JD, et al. Trans fat diet induces abdominal obesity and changes in insulin sensitivity in monkeys. Obesity (Silver Spring). 2007; 15(7):1675–1684. [PubMed: 17636085]
13. Cann JA, Kavanagh K, Jorgensen MJ, Mohanan S, Howard TD, Gray SB, et al. Clinicopathologic characterization of naturally occurring diabetes mellitus in vervet monkeys. Veterinary pathology. 2010; 47(4):713–718. [PubMed: 20460450]
14. Kavanagh K, Wylie AT, Tucker KL, Hamp TJ, Gharaibeh RZ, Fodor AA, et al. Dietary fructose induces endotoxemia and hepatic injury in calorically controlled primates. American Journal of Clinical Nutrition. 2013; 98(2):349–357. [PubMed: 23783298]
15. Bonora E, Targher G, Alberiche M, Bonadonna RC, Saggiani F, Zenere MB, et al. Homeostasis model assessment closely mirrors the glucose clamp technique in the assessment of insulin

sensitivity: studies in subjects with various degrees of glucose tolerance and insulin sensitivity. Diabetes Care. 2000; 23(1):57–63. [PubMed: 10857969]

16. Aron-Wisnewsky J, Tordjman J, Poitou C, Darakhshan F, Hugol D, Basdevant A, et al. Human adipose tissue macrophages: m1 and m2 cell surface markers in subcutaneous and omental depots and after weight loss. J Clin Endocrinol Metab. 2009; 94(11):4619–4623. [PubMed: 19837929]
17. Wagner JE, Kavanagh K, Ward GM, Auerbach BJ, Harwood HJ Jr, Kaplan JR. Old world nonhuman primate models of type 2 diabetes mellitus. ILAR J. 2006; 47(3):259–271. [PubMed: 16804200]
18. Colman RJ, Beasley TM, Kemnitz JW, Johnson SC, Weindruch R, Anderson RM. Caloric restriction reduces age-related and all-cause mortality in rhesus monkeys. Nature communications. 2014; 5:3557.
19. Jorgensen MJ, Aycock ST, Clarkson TB, Kaplan JR. Effects of a Western-type diet on plasma lipids and other cardiometabolic risk factors in African green monkeys (Chlorocebus aethiops sabaeus). Journal of the American Association for Laboratory Animal Science : JAALAS. 2013; 52(4):448–453. [PubMed: 23849442]
20. Voruganti VS, Jorgensen MJ, Kaplan JR, Kavanagh K, Rudel LL, Temel R, et al. Significant genotype by diet (G × D) interaction effects on cardiometabolic responses to a pedigree-wide, dietary challenge in vervet monkeys (Chlorocebus aethiops sabaeus). American journal of primatology. 2013; 75(5):491–499. [PubMed: 23315630]
21. Dalmas E, Toubal A, Alzaid F, Blazek K, Eames HL, Lebozec K, et al. Irf5 deficiency in macrophages promotes beneficial adipose tissue expansion and insulin sensitivity during obesity. Nat Med. 2015; 21(6):610–618. [PubMed: 25939064]
22. Karelis AD, Faraj M, Bastard JP, St-Pierre DH, Brochu M, Prud'homme D, et al. The metabolically healthy but obese individual presents a favorable inflammation profile. J Clin Endocrinol Metab. 2005; 90(7):4145–4150. [PubMed: 15855252]
23. Kloting N, Fasshauer M, Dietrich A, Kovacs P, Schon MR, Kern M, et al. Insulin-sensitive obesity. American journal of physiology Endocrinology and metabolism. 2010; 299(3):E506–E515. [PubMed: 20570822]
24. Esser N, L'Homme L, De Roover A, Kohnen L, Scheen AJ, Moutschen M, et al. Obesity phenotype is related to NLRP3 inflammasome activity and immunological profile of visceral adipose tissue. Diabetologia. 2013; 56(11):2487–2497. [PubMed: 24013717]
25. Mitchell T, Chacko B, Ballinger SW, Bailey SM, Zhang J, Darley-Usmar V. Convergent mechanisms for dysregulation of mitochondrial quality control in metabolic disease: implications for mitochondrial therapeutics. Biochemical Society transactions. 2013; 41(1):127–133. [PubMed: 23356271]
26. Zhou R, Yazdi AS, Menu P, Tschopp J. A role for mitochondria in NLRP3 inflammasome activation. Nature. 2011; 469(7329):221–225. [PubMed: 21124315]
27. Hotamisligil GS, Peraldi P, Budavari A, Ellis R, White MF, Spiegelman BM. IRS-1-mediated inhibition of insulin receptor tyrosine kinase activity in TNF-alpha- and obesity-induced insulin resistance. Science. 1996; 271(5249):665–668. [PubMed: 8571133]
28. Choo HJ, Kim JH, Kwon OB, Lee CS, Mun JY, Han SS, et al. Mitochondria are impaired in the adipocytes of type 2 diabetic mice. Diabetologia. 2006; 49(4):784–791. [PubMed: 16501941]
29. Kusminski CM, Bickel PE, Scherer PE. Targeting adipose tissue in the treatment of obesity-associated diabetes. Nat Rev Drug Discov. 2016; 15(9):639–660. [PubMed: 27256476]
30. Mottillo EP, Desjardins EM, Crane JD, Smith BK, Green AE, Ducommun S, et al. Lack of Adipocyte AMPK Exacerbates Insulin Resistance and Hepatic Steatosis through Brown and Beige Adipose Tissue Function. Cell Metab. 2016; 24(1):118–129. [PubMed: 27411013]
31. Liu M, Aneja R, Sun X, Xie S, Wang H, Wu X, et al. Parkin regulates Eg5 expression by Hsp70 ubiquitination-dependent inactivation of c-Jun NH2-terminal kinase. J Biol Chem. 2008; 283(51): 35783–35788. [PubMed: 18845538]
32. Chichester L, Wylie AT, Craft S, Kavanagh K. Muscle Heat Shock Protein 70 Predicts Insulin Resistance With Aging. The journals of gerontology Series A, Biological sciences and medical sciences. 2014

33. Drew BG, Ribas V, Le JA, Henstridge DC, Phun J, Zhou Z, et al. HSP72 is a mitochondrial stress sensor critical for Parkin action, oxidative metabolism, and insulin sensitivity in skeletal muscle. Diabetes. 2014; 63(5):1488–1505. [PubMed: 24379352]

34. Kavanagh K, Wylie AT, Chavanne TJ, Jorgensen MJ, Voruganti VS, Comuzzie AG, et al. Aging does not reduce heat shock protein 70 in the absence of chronic insulin resistance. The journals of gerontology Series A, Biological sciences and medical sciences. 2012; 67(10):1014–1021. [PubMed: 22403054]

35. Kavanagh K, Flynn DM, Jenkins KA, Zhang L, Wagner JD. Restoring HSP70 deficiencies improves glucose tolerance in diabetic monkeys. American journal of physiology Endocrinology and metabolism. 2011; 300(5):E894–E901. [PubMed: 21325107]

36. Altshuler-Keylin S, Shinoda K, Hasegawa Y, Ikeda K, Hong H, Kang Q, et al. Beige Adipocyte Maintenance Is Regulated by Autophagy-Induced Mitochondrial Clearance. Cell Metab. 2016; 24(3):402–419. [PubMed: 27568548]

37. Schneider H, Dietrich ES, Venetz WP. Trends and stabilization up to 2022 in overweight and obesity in Switzerland, comparison to France, UK, US and Australia. Int J Environ Res Public Health. 2010; 7(2):460–472. [PubMed: 20616985]

What is already known

- Obesity can exist with or without accompanying metabolic disease as defined by current arbitrary cutoff values for diabetes and cardiovascular disease risk factors.
- Healthy obesity leads to protection, or more likely a delay, from the progression towards being classified as high risk for cardiometabolic disease.
- Deranged mitochondrial function and degradation and immune cell shifts in subcutaneous adipose can replicate some aspects of metabolic disease in obese rodent models.

What does this study add

- Characterization of a large animal model for preclinical investigations of obesity and cardiometabolic health which is superior to rodents as adipose does not brown as readily, overt Type 2 diabetes, heart failure and relevant atherosclerotic lesions develop spontaneously with pathological features that resemble human disease.
- Subcutaneous adipose macrophage polarization differentiates by Metabolic Syndrome status such that unhealthy obesity is associated with deficient M2 alternatively activated macrophage numbers.
- Proteins involved in mitochondrial quality control, but not abundance, were deficient in unhealthy obese subcutaneous adipose tissue.

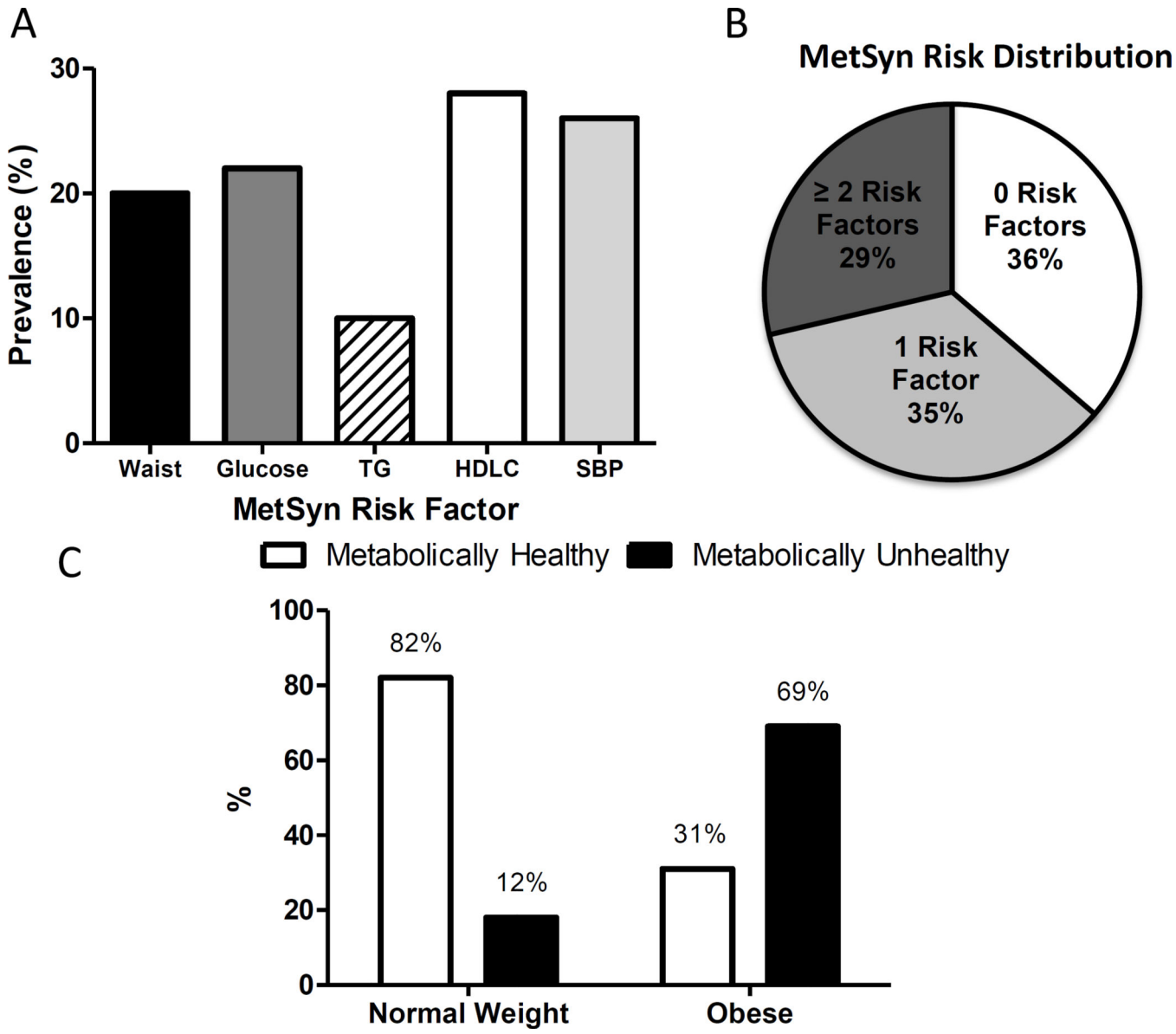

Figure 1.

A) Prevalence of older monkeys with positive metabolic syndrome risk criteria despite the consumption of a low fat, low simple carbohydrate diet and free opportunity for physical activity. B) Distribution of metabolic syndrome risk factor clustering in 171 vervet monkeys. C) Prevalence of cardiometabolic abnormality by adiposity status (normal or enlarged waist circumference) of vervet monkeys.

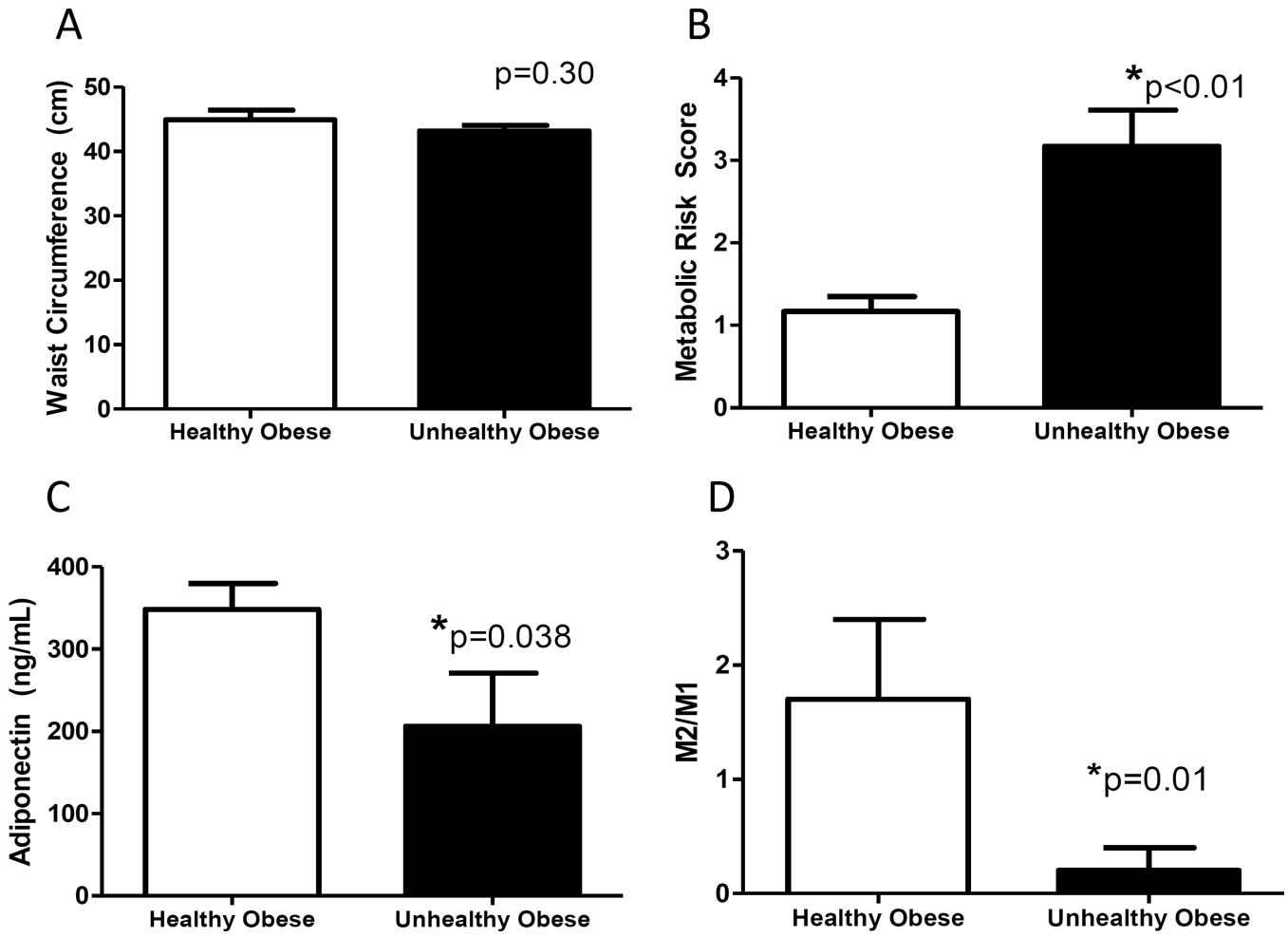

Figure 2.

Characteristics of metabolically healthy and unhealthy obese monkeys selected randomly from the subset of the population matched on age and BW for fat biopsy (additional data in Table 2). Despite comparable age and waist circumferences (Panel A), monkeys selected were unhealthy as defined by high metabolic syndrome risk scores (Panel B), which was accompanied by reductions in circulating adiponectin concentrations (Panel C). Panel D: Metabolically unhealthy obese monkeys had shifts in the classically and alternatively activated macrophage populations (M1 and M2 respectively) in subcutaneous fat, with the unhealthy monkeys demonstrating a more pro-inflammatory ratio (n=6/group). All panels show group average with standard error of the means.

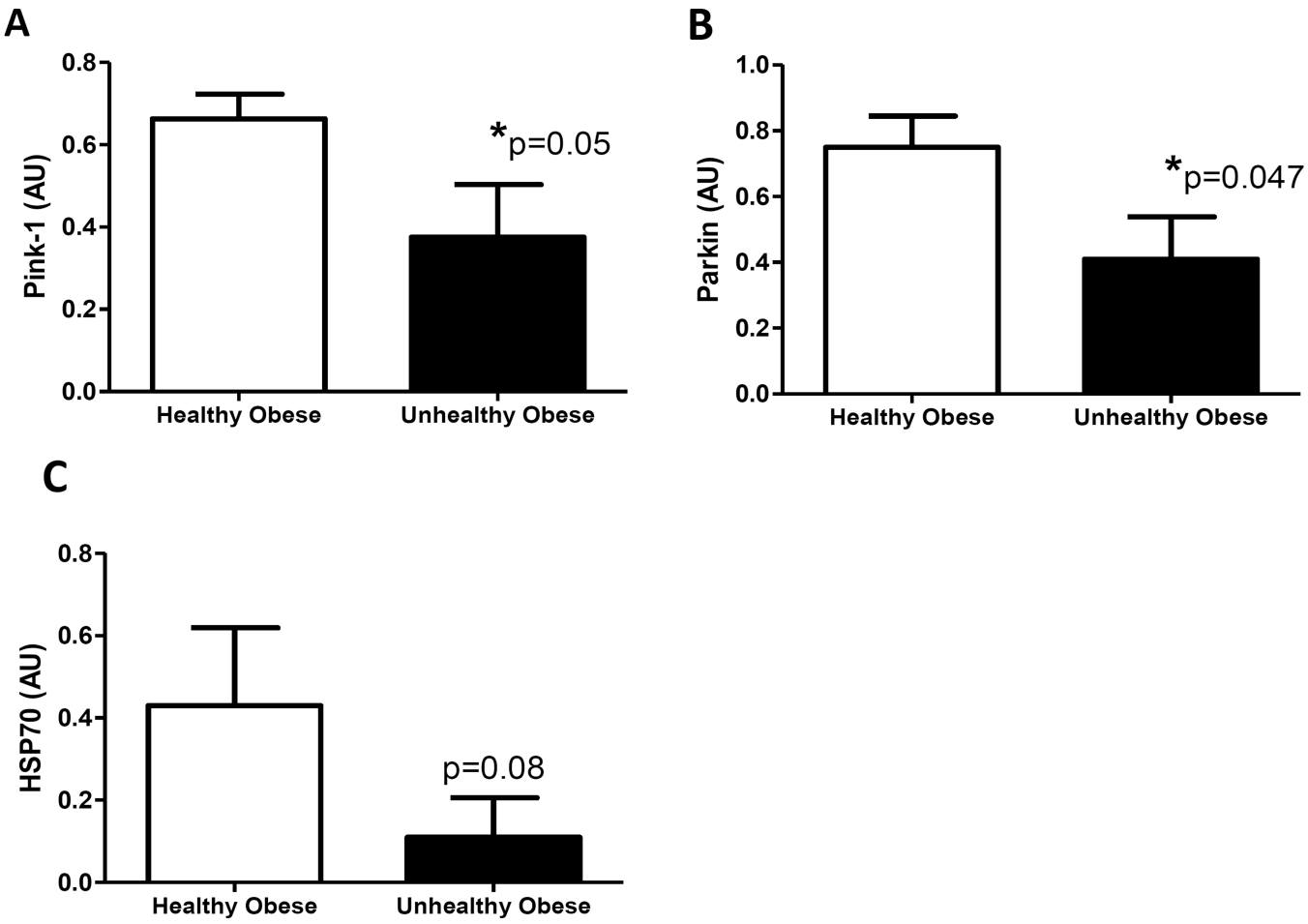

Figure 3.

Mitophagy-related proteins are reduced in subcutaneous fat of obese monkeys classified as metabolically unhealthy. We observe a 43% lower pink-1 (Panel A), 44% lower parkin (Panel B), and 73% lower heat shock protein (HSP)70 (Panel C) in unhealthy obese monkeys as compared to healthy obese monkeys (n=6/group). All panels show group average with standard error of the means.

Table 1

Characteristics of vervet monkeys screened for metabolic syndrome criteria biomarkers (*).

	Healthy Lean	Unhealthy Lean	Healthy Obese	Unhealthy Obese	p-value
N (%♂)	111 (11%)	25 (12%)	11 (9.01%)	24 (8.33%)	
Age (yrs)	16.1 (4.28)	16.0 (4.35)	15.7 (3.83)	16.0 (3.33)	0.98
Waist* (cm)	35.2 (2.82)^{a}	35.6 (2.79)^{a}	43.9 (2.74)^{b}	44.7 (2.86)^{b}	<0.001
Glucose* (mg/dL)	77.6 (20.6)^{a}	115 (36.1)^{b}	86.6 (25.4)^{c}	115 (25.8)^{b}	<0.001
TG* (mg/dL)	64.3 (1.57)^{a}	82.1 (7.49)^{b}	68.9 (4.93)^{ab}	89.9 (9.40)^{bc}	<0.001
HDLC* (mg/dL)	57.9 (1.12)^{a}	50.7 (2.50)^{b}	58.3 (1.89)^{ab}	59.2 (4.81)^{ab}	0.04
SBP* (mmHg)	115 (2.22)^{a}	137 (5.00)^{b}	111 (4.30)^{a}	132 (6.61)^{a}	<0.001
MetSyn Score	0.44 (0.05)^{a}	2.16 (0.09)^{b}	1.54 (0.10)^{c}	3.18 (0.12)^{d}	<0.001
TPC/HDLC	2.64 (0.42)^{a}	2.96 (0.65)^{a}	2.70 (0.33)^{a}	4.06 (3.11)^{b}	<0.001
TPC (mg/dL)	148 (26.3)^{a}	142 (29.3)^{a}	154 (27.0)^{a}	182 (55.8)^{b}	0.002
BW (kg)	5.42 (0.84)^{a}	5.59 (1.06)^{a}	7.20 (1.17)^{b}	7.38 (0.85)^{b}	<0.001
HOMA	4.71 (3.09)^{a}	8.93 (6.70)^{b}	7.90 (4.57)^{b}	13.9 (8.03)^{c}	<0.001
Insulin (μIU/mL)	24.4 (1.43)^{a}	32.0 (4.62)^{a}	35.8 (3.09)^{b}	48.7 (7.83)^{b}	<0.001

A score for metabolic syndrome risk (MetSyn Score) is the number of criteria met (range 0–5). Means with standard errors of the means shown in parentheses.

Unlike superscripted letters indicate significant differences between groups.

Table 2

Additional phenotypic and subcutaneous adipose tissue characteristics of randomly selected MHO and MUO vervet monkeys (n=6/group). UCP3 is used as a marker for browning of fat, CD68 identifies activated macrophages (M1), and CD163 identifies alternatively activated macrophages (M2).

		Healthy Obese	Unhealthy Obese	p-value
Phenotypic Measures	**Age (yrs)**	16.6 (1.08)	18.0 (1.82)	0.52
	BW (kg)	6.99 (0.37)	6.55 (0.43)	0.23
	Glucose (mg/dL)	76.6 (6.54)	119 (12.4)	0.006
	Insulin (uIU/mL)	24.7 (2.86)	43.8 (10.5)	0.06
	HOMA (AU)	4.76 (0.80)	12.5 (2.61)	0.009
	SBP (mmHg)	107 (12.5)	126 (13.1)	0.15
	TPC (mg/dL)	145 (6.80)	165 (33.0)	0.28
	HDLC (mg/dL)	54.0 (0.55)	49.3 (7.08)	0.26
	TG (mg/dL)	67.5 (6.47)	66.8 (8.94)	0.47
	CRP (ng/mL)	2.07 (0.622)	1.58 (0.650)	0.56
	IL-6 (pg/mL)	9.89 (4.96)	8.66 (2.53)	0.81
SQ Adipose Measures	**UCP3 (AU)**	0.317 (0.079)	0.281 (0.081)	0.38
	Adipocyte diameter (μm)	127 (4.19)	122 (7.34)	0.60
	CD68^{+ve} (n/HPF)	3.93 (0.99)	4.93 (0.84)	0.42
	CD163^{+ve} (n/mm^2)	4.6×10^{-5} (1.8×10^{-5})	1.4×10^{-5} (0.9×10^{-5})	0.03

Means with standard errors of the means shown in parenthesis. HPF=high powered field

Table 3

Subcutaneous adipose tissue mitochondrial protein quantifications by immunoblot of biopsy tissue collected from MHO and MUO vervet monkeys.

	Mitochondrial Marker	Healthy Obese (n=6)	Unhealthy Obese (n=6)	p-value
FIS1	Fission	0.089 (0.021)	0.131 (0.015)	0.14
DRP1	Fission	0.433 (0.054)	0.246 (0.082)	0.04
OPA1	Fusion	0.346 (0.083)	0.236 (0.018)	0.22
Mfn1	Fusion	0.151 (0.022)	0.084 (0.016)	0.03
Mfn2	Fusion	0.115 (0.052)	0.067 (0.038)	0.48
Porin	Content	0.79 (0.02)	0.66 (0.05)	0.02
COXIV	Content	0.839 (0.194)	0.753 (0.160)	0.74
PGC1	Biogenesis	0.540 (0.260)	0.316 (0.061)	0.42
SIRT1	Biogenesis	0.266 (0.119)	0.134 (0.031)	0.15
SIRT3	Biogenesis	0.428 (0.138)	0.307 (0.110)	0.25
TFAM	Biogenesis	0.439 (0.075)	0.317 (0.096)	0.17

Means with standard errors of the means shown in parentheses.